Fatigue mechanisms in ultrafine-grained copper

P. Lukáš*, L. Kunz, M. Svoboda

Institute of Physics of Materials, Academy of Sciences of the Czech Republic, Žižkova 22, 616 62 Brno, Czech Republic

Received 23 January 2009, received in revised form 18 February 2009, accepted 19 February 2009

Abstract

Fatigue behaviour of ultrafine-grained (UFG) copper produced by equal-channel angular pressing (ECAP) was studied at room temperature and at depressed temperatures of 173 K and 103 K. Effect of material purity was investigated at room temperature on UFG coppers of three substantially different purities. Temperature sensitivity of fatigue strength and cyclic flow stress of UFG copper is lower than that of copper with conventional grain size. Fatigue strength strongly depends on purity at low stress amplitudes and is independent of it at high stress amplitudes. No substantial changes of microstructure were detected after cyclic loading. Surface fatigue slip markings along the traces of the shear planes of the ECAP process were observed. Two concurrent mechanisms of cyclic plastic deformation in UFG copper are proposed: (i) bulk mechanism consisting of irreversible movement of dislocations and (ii) surface mechanism operating in the surface layer consisting of grain boundary sliding along shear planes of ECAP process.

Key words: ultrafine-grained copper, fatigue strength, cyclic plasticity, effect of purity, effect of temperature, stability of UFG structure

1. Introduction

It was unequivocally proved in the last two decades that severe plastic deformation is an effective way how to increase strength and hardness of metals without substantial loss of their ductility. This especially concerns materials prepared by the method of equal-channel angular pressing (ECAP) producing materials with an ultra-fine grain size of the order of hundreds of nanometres. For example, in the case of commercial pure copper ten ECAP passes resulted in increase of ultimate tensile strength from 275 MPa to 464 MPa with almost negligible loss of ductility; the grain size decreased from the initial 50 μm to 100–300 nm [1, 2].

The fatigue properties of the ultrafine-grained (UFG) metals prepared by the ECAP technique have been studied on quite a large scale. Besides several hundreds of primary articles also a few overview articles have been written [e.g. 3–5]. With a few notable exceptions, the UFG metals were found to exhibit higher fatigue strength than their conventional-grain (CG) counterparts provided the cycling was stress-controlled. For strain-controlled cycling the situation is usually reversed. In comparison to CG metals, the UFG metals have usually a lower resistance against fatigue crack propagation. Further details of fatigue behaviour vary from material to material. The originally very promising expectation of broad engineering application of UFG materials has been cooled down by the fact that highly deformed microstructures can be unstable under cyclic loading. The understanding of microstructural stability and its response to cyclic loading is crucial for engineering applications. Due to the danger of instabilities, which increases with increasing temperature, the UFG materials prepared by ECAP technique are predestined for use at ambient and depressed temperatures. Monotonic tests carried out at temperatures down to 77 K on ultrafine-grained metals (Cu, Ni and Al-4Cu-0.5Zr reported in [6] and Al reported in [7]) prepared by ECAP technique show that the temperature sensitivity of tensile properties of UFG metals is significantly higher than that typical for annealed fcc polycrystalline metals. On the other hand, nothing is known on the temperature sensitivity of fatigue properties of UFG metals.

*Corresponding author: tel.: +420 541 212 286; fax: +420 541 212 301; e-mail address: lukas@ipm.cz

Table 1. Characteristics of UFG coppers

Purity (pct)	No. of passes	Route	Label	Specimen
99.5	4	C	99.5/C/4	$7 \times 3\,mm^2$
99.5	6	C	99.5/C/6	$7 \times 3\,mm^2$
99.9	8	B_c	99.9/B_c/8	ø 6 or 7 mm
99.9998	6	B_c	99.9998/B_c/6	$7 \times 3\,mm^2$
99.9998	6	C	99.9998/C/6	$7 \times 3\,mm^2$

Out of the UFG metals, the mostly often used one for fatigue studies has been a model material, namely copper. UFG copper has been investigated both from the point of view of the macroscopic fatigue properties and from the point of view of the structural and microstructural changes taking place during cycling. Nevertheless, there are crucial differences between the fatigue life data of UFG copper obtained in different laboratories. There is also no broader agreement on the underlying reasons. Fatigue properties and fatigue damage of copper with conventional grain size (typically of the order of tens of microns) have been very extensively studied for at least last fifty years. As for CG copper, there are no substantial differences in fatigue data and there is a more or less general agreement on the fatigue mechanisms.

The aim of this paper is to present results on the effect of temperature and purity on the fatigue performance of UFG copper, juxtapose them to the knowledge on the fatigue of CG copper and to propose mechanisms of fatigue process in UFG copper.

2. Experimental

Copper of 99.9 % purity was used for the investigation of the effect of low temperature. Cylindrical samples were processed by ECAP technique by 8 passes and route B_c. Fatigue experiments were conducted using cylindrical specimens with the gauge section diameter of 6 or 7 mm in two testing systems under controlled load. A servo-hydraulic pulser equipped with a clip-on extensometer and data acquisition system was used for tests, during which the hysteresis loops were recorded at preset numbers of cycles. The frequency of cycling was set to be either 1 or 5 or 10 Hz, the loading was sinusoidal and load symmetrical. During recording the frequency was decreased to 0.1 Hz. The plastic strain amplitude was taken as the half-width of the hysteresis loop. A resonant fatigue machine operating at frequency either 124 or 213 Hz (in dependence on the gauge section diameter and length) was used mainly for long-life tests; no hysteresis loops were recorded. The tests were carried out at room temperature (295 K tests) and at low temperatures (173 K tests and 103 K tests). The 295 K tests were run in laboratory air, the low temperature tests in nitrogen vapors. Gauge length of specimens predestined for surface observations by scanning electron microscope (SEM) was carefully electrochemically polished.

To study the effect of purity, two more UFG coppers of extremely different purities (99.5 and 99.9998 %) were used besides the above mentioned UFG copper of purity 99.9 %. Materials were processed by routes B_c and C. Flat specimens with $7 \times 3\,mm^2$ cross-section were machined from the billets. Main data are shown in Table 1.

Grain morphology was observed both in virgin material and in cycled specimens by electron back scattering diffraction (EBSD) technique in SEM. Quality image maps and orientation maps were processed by Oxford INCA crystal EBSD system in JEOL 6460 SEM. The corresponding grain maps were constructed as regions having orientation range within 5 degrees. For grain size characterization equivalent circle diameter was used. Transmission electron microscopy (TEM) on thin foils was used for observation of dislocation structures.

3. Results and discussion

3.1. Effect of temperature

Examples of cyclic stress-strain response of UFG copper are shown in Fig. 1 for room temperature (295 K) and for 103 K. The plastic strain amplitude is plotted in dependence on the relative number of loading cycles, N/N_f, where N_f is number of cycles to failure. Each curve is marked by the stress amplitude at which the test was run. It can be clearly seen that the specimens cycled at higher stress amplitudes soften during the prevailing part of the lifetime. At the very beginning of the high amplitude 103 K tests a quick hardening can be observed. As the hardening/softening curves do not exhibit saturation behaviour, the cyclic stress-strain curves can be defined only conventionally on the basis of the stress and strain values corresponding to one half of the fatigue life. The experimental data obtained for all studied temperatures are presented in Fig. 2. Part of the

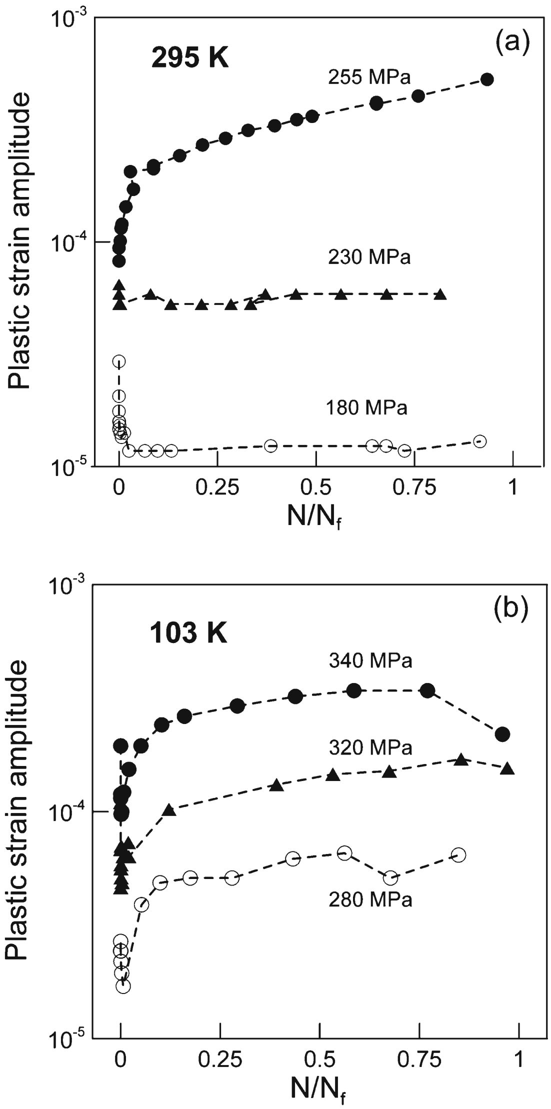

Fig. 1. Cyclic hardening/softening curves of UFG copper (99.5 %): (a) 295 K and (b) 103 K.

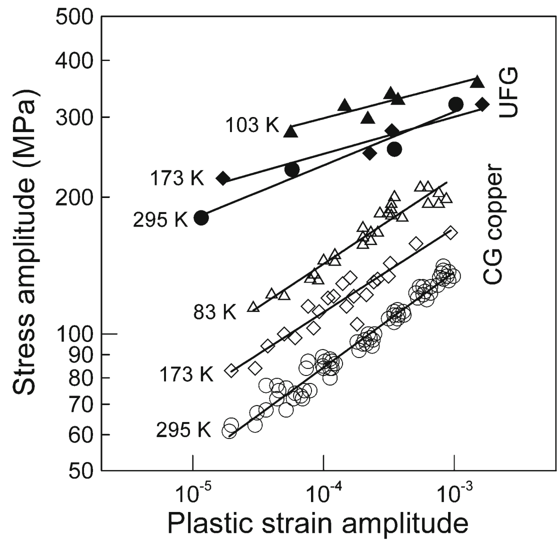

Fig. 2. Effect of temperature on cyclic stress-strain curves of UFG and CG coppers.

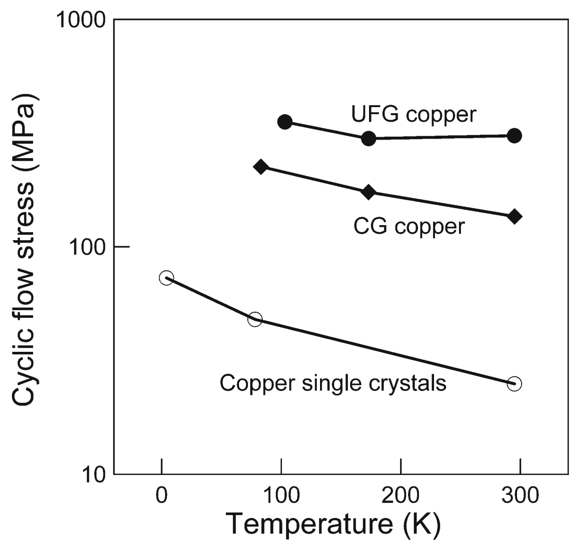

Fig. 3. Temperature sensitivity of cyclic flow stress.

data for UFG copper cycled at 173 K was taken from [8]. Besides the data for UFG copper, also the comparable data obtained on CG copper (published in our earlier paper [9]) are juxtaposed for comparison. It can be seen that the effect of temperature on the cyclic stress-strain curves in the case of UFG copper is lower than that in the case of CG copper. Cyclic flow stress corresponding to the plastic strain amplitude of 0.001 was chosen for the quantification of the temperature sensitivity. Its dependence on temperature is shown in Fig. 3 together with the analogical dependence for CG copper [9]. The values of plateau stress of copper single crystals taken from the paper by Basinski et al. [10] are plotted too. It can be seen that the temperature sensitivity of cyclic flow stress is highest for the copper single crystals, medium for the CG copper and very low for the UFG copper. Figure 4 shows the effect of temperature on the S-N curves. Here again, the temperature sensitivity of UFG copper is lower than that of CG copper.

Application of TEM and EBSD methods to the examination of cycled specimens yield the results that at all the examined temperatures there is a slight effect of cycling on the microstructure consisting of a certain "purification" of the grain interiors and related small apparent increase of the "EBSD grain size". This claim can be elucidated with the help of the following micrographs. Figure 5 presents two TEM micrographs, one corresponding to virgin material (Fig. 5a) and one taken on the foil prepared from the specimen cycled

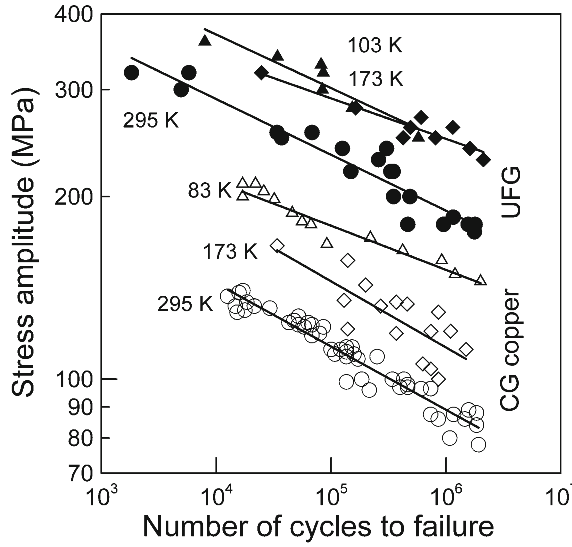

Fig. 4. Effect of temperature on *S-N* curve of UFG and CG coppers.

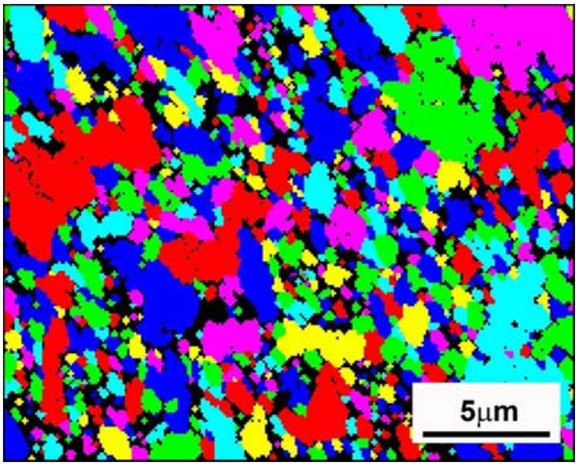

Fig. 6. EBSD micrograph of grain structure in specimen cycled at 173 K.

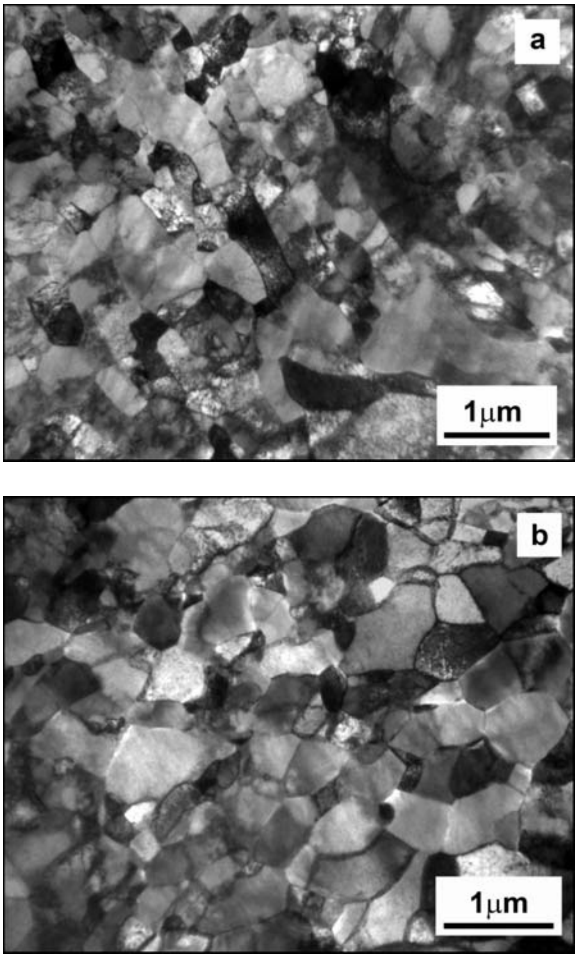

Fig. 5. Effect of cycling at 173 K on TEM structure of UFG copper: (a) before cycling, (b) after cycling at stress amplitude of 320 MPa for 2.48×10^4 cycles.

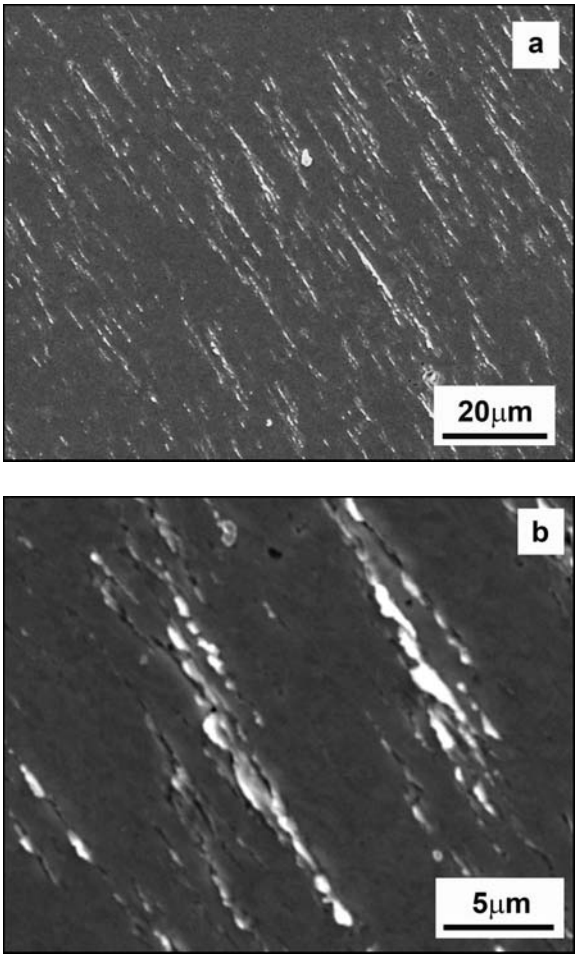

Fig. 7. Surface slip markings after cycling at 173 K: (a) family of fatigue slip markings along traces of ECAP shear plane, (b) alternating extrusions and intrusions.

at 173 K (Fig. 5b). In both the cases the "TEM grain size" is about 300 nm. Examination of a large number of micrographs of this type shows that the density of dislocations within the grains in cycled specimens is somewhat lower than that in virgin specimens. This holds especially at very high stress amplitudes. An EBSD micrograph taken on the specimen after cycling at 173 K is shown in Fig. 6. This micrograph is depicted in the "grain map" mode with the threshold angle of 5°. The "EBSD grain size" in this case is 780 nm. The difference between the EBSD micrographs of virgin material and micrographs of specimens after cyclic loading lies in the "EBSD grain size". The typical "EBSD grain size" for virgin material is about 700 nm. This result indicates that during purification of the grain interiors shown in Fig. 5 some low-angle boundaries decrease their misorientation below 5 degrees.

A typical SEM micrograph showing surface slip markings produced by cycling at low temperatures is shown in Fig. 7. Well developed family of fatigue slip markings following the traces of the ECAP shear planes on the surface can be seen in Fig. 7a. Their average length substantially exceeds the average grain size of material. Alternating extrusions and intrusions can be seen at higher magnification in Fig. 7b. Here thin tongues of a height up to several microns strike out from the surface. The fatigue markings on the surface of specimens cycled at room temperature are of the same type [11].

3.2. Effect of purity

The effect of purity on the fatigue strength of UFG copper is documented in Fig. 8 on *S-N* data obtained in different laboratories. The uppermost *S-N* curve summarizes results [8, 11] obtained on UFG copper of purity 99.9 %. The lowermost thick *S-N* curve characterizing the scatter band of experimental data is based on a great number of *S-N* points on CG copper as summarized by Murphy [12] in 1981; later data fit into this band as well. Important point is that the *S-N* data of CG copper are rather insensitive to material purity and grain size. Comparing the uppermost and the lowermost curves in Fig. 8, it is clear that the fatigue strength of UFG copper of purity 99.9 % is by a factor of about 2 higher than that of CG copper in the very broad region of fatigue lives. Data obtained on UFG copper of purity 99.99 % [3, 13, 14] exhibit improvement over the CG data only in the LCF and HCF regions. Their extrapolation suggests that in VHCF region the fatigue strength of UFG Cu drops to that of CG Cu.

The *S-N* curves of UFG coppers of three substantially different purities tested in the frame of the present programme are shown in Fig. 9. The tests were carried out in one laboratory under the same testing conditions. Thus the effect of variances in testing

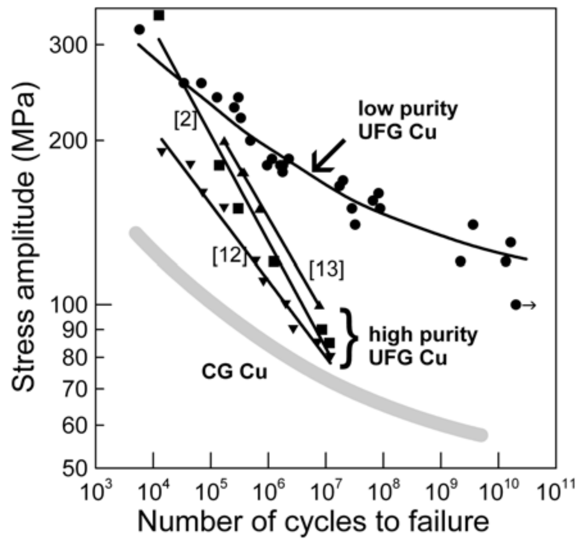

Fig. 8. Effect of purity on *S-N* curves of UFG copper. Survey of literary data.

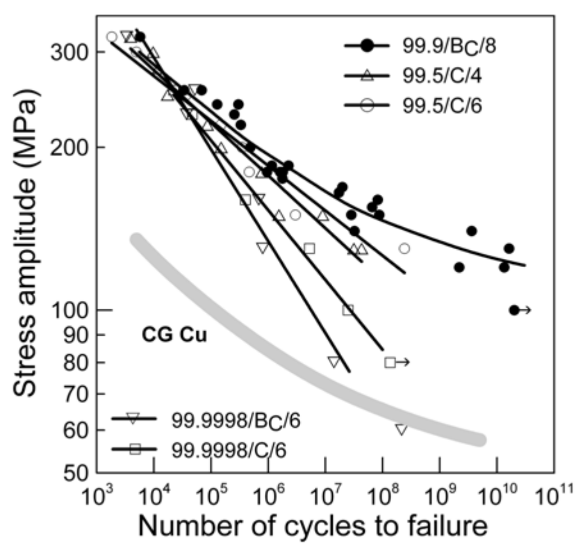

Fig. 9. Effect of purity on *S-N* curves of UFG copper. Experimental data of this work.

procedures (except of the different specimen shape) is eliminated. It can be seen that the data presented in Fig. 9 confirm the main conclusion of Fig. 8, i.e. that the fatigue strength of high purity UFG copper is lower than that of lower purity UFG copper. Figure 9 also shows that the ECAP route affects fatigue strength as well (compare curves 99.9998/B_c/6 and 99.9998/C/6). Both the effects (purity and route) are more pronounced for low stress amplitudes. At high stress amplitudes corresponding to lifetimes below 10^4 cycles the effects are practically wiped off. The effect of purity on the *S-N* curve was by several authors attributed to lower stability of grain structure in UFG

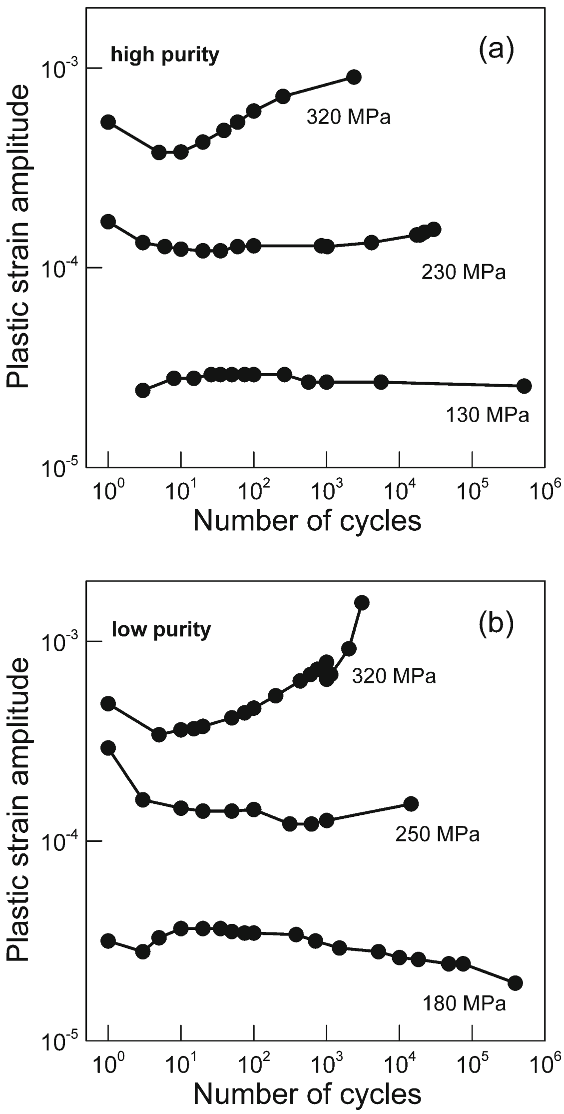

Fig. 10. Cyclic hardening/softening curves of UFG coppers: (a) $99.9998/B_c/6$, (b) $99.5/C/4$.

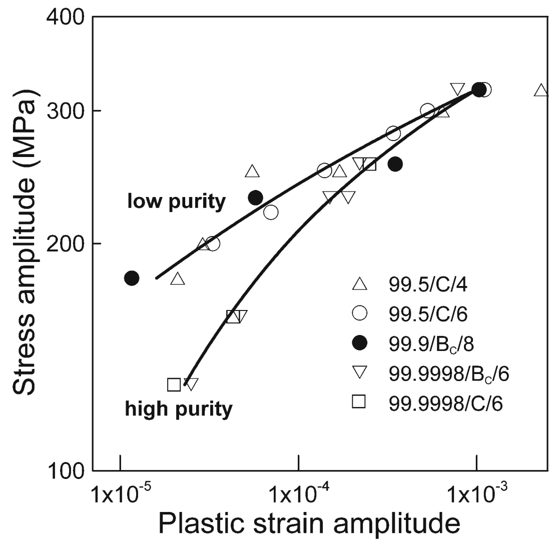

Fig. 11. Cyclic stress-strain curves of UFG coppers.

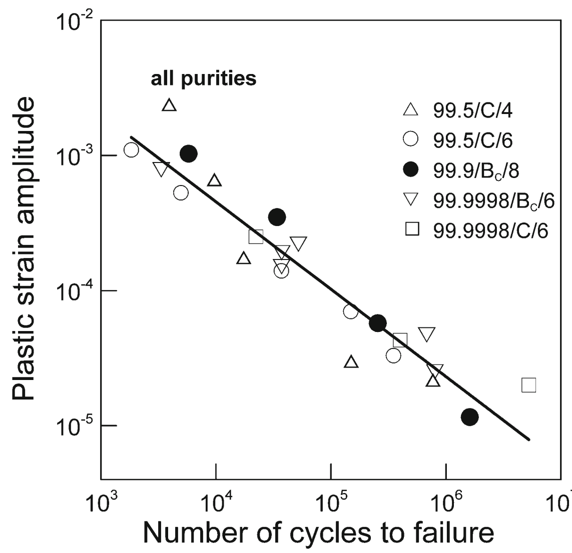

Fig. 12. Manson-Coffin plot of UFG coppers.

copper of higher purity, i.e. to grain coarsening. Extensive investigation of microstructure carried out in the present study did not reveal any grain structure instability in cycled UFG coppers. Irrespective of the purity, the TEM micrographs were of the type shown in Fig. 5 with the "TEM grain size" of about 300 nm and the EBSD micrographs were of the type shown in Fig. 6 with the "EBSD grain size" of about 700–800 nm. In other words, no grain coarsening has ever been detected.

The shape of the cyclic hardening/softening curves does not depend on the purity. Examples are shown in Fig. 10. The plastic strain amplitude is plotted in dependence on the number of cycles. It can be seen that the specimens cycled at higher stress amplitudes soften during the prevailing part of the lifetime, while the specimens cycled at lower amplitudes harden. This means that even in severely deformed metal there is still a potential for further hardening. The cyclic stress-strain curves defined conventionally on the basis of the stress and strain values corresponding to one half of the fatigue life are presented in Fig. 11 for all five investigated UFG coppers. The data can be well separated into two groups according to the purity. The cyclic stress-strain curve for low purity coppers lies above the curve for high purity coppers. The difference decreases with increasing stress amplitude. Here again the effect of purity is practically wiped off at high stress amplitudes. No measurable differences were found between the coppers of the same purity treated by different ECAP routes. Combination of the cyclic stress-strain curves (Fig. 11) with the *S-N* curves (Fig. 10) makes it possible to plot the fatigue life in terms of Manson-Coffin diagram. This diagram is shown in Fig. 12. It can be seen that fatigue life data of all the investigated UFG coppers presented in terms of Manson-Coffin plot fall into one narrow scatter band. Thus it can be stated that the plastic strain amplitude is a unifying parameter as regards lifetime prediction.

Appearance of slip markings observed by SEM on surface of cycled specimens is shown in Fig. 13 for high purity (a) and low purity UFG coppers (b). Fatigue slip markings always follow the traces of the ECAP shear planes. The average length of the alternating extrusions and intrusions substantially exceeds the average grain size of material. The same was found for all investigated UFG coppers.

3.3. Mechanisms

The main experimental findings can be summarized as follows:

(i) The cyclic stress-strain curve of UFG copper is slightly temperature sensitive. The temperature dependence of the cyclic flow stress is highest for the copper single crystals, medium for the CG copper and lowest for the UFG copper.

(ii) The *S-N* curve is temperature dependent, but the temperature sensitivity for UFG copper is lower than that for CG copper.

(iii) The *S-N* curve of UFG copper depends on the purity in such a way that this dependence is very strong for low stress amplitudes and practically none for very high stress amplitudes corresponding to LCF region.

(iv) Similarly to the *S-N* curve, the cyclic stress-strain curve of UFG copper depends on the purity in such a way that this dependence is strong for low stress amplitudes and practically none for very high stress amplitudes corresponding to LCF region.

(v) The grain structure of UFG coppers is stable and undergoes only very marginal changes (detected by EBSD and TEM) during cycling at all testing temperatures.

(vi) The appearance of fatigue markings on the surface of cycled UFG copper does not detectably depend on the purity and on the temperature of cycling.

To explain consistently the observed effects of purity and temperature on the fatigue behaviour of UFG copper, two mechanisms of cyclic plastic deformation have to be taken into account:

(i) bulk dislocation mechanism taking place in the whole loaded volume; this mechanism produces the major part of the measured plastic strain amplitude and

(ii) localized mechanism taking place in the surface layer and leading to formation of surface fatigue markings and to initiation of microcracks; this mechanism contributes only marginally to the plastic strain amplitude measured over the gauge length, but affects substantially the fatigue lifetime.

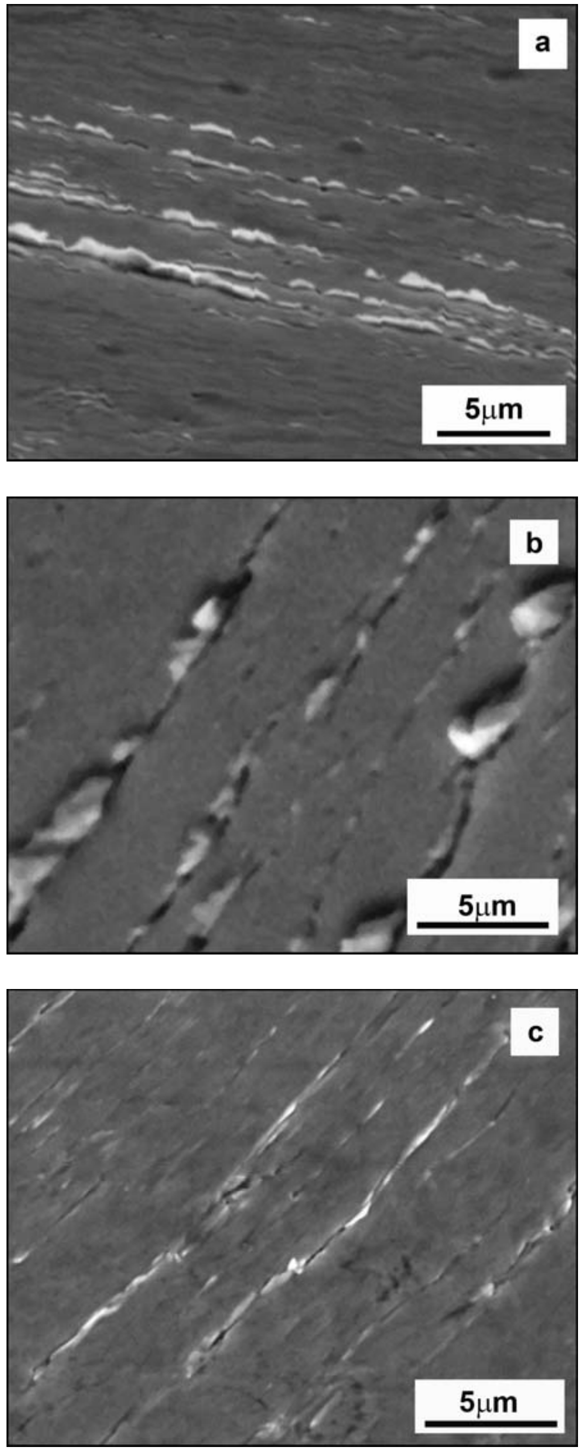

Fig. 13. Fatigue slip markings on surface of cycled specimens of purity 99.9998 % (a), 99.9 % (b) and 99.5 % (c).

The first mechanism depends on purity simply because impurities hinder motion of dislocations. The first mechanism depends only weakly on temperature. The second mechanism depends strongly both on purity and on temperature. The bulk mechanism is a dislocation mechanism consisting of irreversible movement of dislocations and manifesting itself by non-zero width of hysteresis loops and by the "purification" of the grain interiors (see TEM results) and by the fact that some low-angle boundaries decrease their disorientation (see EBSD results). The localized mechanism, resulting in formation of surface fatigue markings is related to the grain boundary (GB) sliding. Highly non-equilibrium GBs in UFG materials were shown to slide easily in the case of tensile deformation [15]. Similar behaviour can be expected in cyclic deformation [16].

To discuss the effects of purity and temperature on the cyclic stress-strain curve it is convenient to use the old concept of splitting the stress needed for motion of dislocations (in "bulk" mechanism) into two components, internal stress σ_{i} and effective stress σ_{ef} [17]. The effective stress (meaning "effective" on the short-range mechanisms) is related to the thermally activated processes and thus depends on the strain rate $\dot{\varepsilon}$ and on the temperature T. The internal stress (related to the long-range stress fields) depends on the dislocation structure which in turn can depend on temperature. Both the stress components are also functions of strain ε. The external stress (in our case of cycling coincident with the stress amplitude) can be written as

$$\sigma = \sigma_{\mathrm{ef}}(\varepsilon,\dot{\varepsilon},T) + \sigma_{\mathrm{i}}(\varepsilon, \mathrm{structure}).$$

It is generally agreed that σ_{ef} stress component in fcc metals is substantially smaller than the σ_{i} component; this holds both for monotonic and cyclic plastic deformation. Moreover, for fcc metals it was many times shown that the dislocation structure produced by cycling strongly depends on test temperature. More exactly, the characteristic size of the dislocation patterning decreases with decreasing temperature. Basinski et al. [10] showed it for the ladder spacing in the persistent slip bands of cycled copper single crystals; Holste [18] proved the same for nickel single crystals. Feltner and Laird [19] found this temperature effect for cell size of polycrystalline copper cycled in low cycle region and Lukáš and Kunz [9] for ladder spacing and vein spacing of polycrystalline copper cycled in high cycle region. In all the quoted cases the cyclic stress was found to be strongly temperature dependent in such a way that the stress amplitude is inversely proportional to the characteristic size of the dislocation patterning. The temperature sensitivity of cyclic flow stress of UFG copper is weak in comparison to that of CG cooper and to copper single crystals (Fig. 3). Due to very limited possibilities for dislocation generation and patterning within the small grains, the cyclic plastic deformation in UFG copper does not lead to any dislocation patterning. Thus the component σ_{i} in the upper equation does not depend on temperature and probably also not on purity. The dependence of the stress-strain curve on temperature and purity can be then attributed mainly to the component σ_{ef}. As this component represents only a small part of the total stress, the temperature and purity dependences of the cyclic flow stress are weak.

The well-developed extrusions and intrusions observed generally on the surface of loaded UFG Cu prove local transfer of matter. This observation indicates that some kind of cooperative grain boundary sliding along the ECAP shear planes is the decisive mechanism for formation of fatigue markings and for the nucleation and propagation of short cracks. In other words, the "localized" mechanism may consist of glide of the whole layers of grains along the ECAP shear planes. It can be expected, that the local direction of the co-operative grain boundary sliding would reflect the microstructure in that sense that in suitable oriented areas having low angle boundaries grain boundary sliding will take place whereas unsuitable oriented areas will serve as local barriers. The concept of the highly localized cooperative grain boundary sliding can be used for explanation of the dependence of the *S-N* curve on purity. Generally it holds for all metals, that microcrack initiation represents only a small part of the total number of cycles to failure in the LCF region and, on the contrary, a substantial part of the total fatigue life in the HCF and VHCF regions. The proportion of the initiation number of cycles increases with decreasing loading amplitude. The *S-N* curves in Fig. 9 look like a flap displaying shortest life for highest purity. It leads to conclusion that the microcrack initiation is easier for high purity UFG copper than for low purity one, while the number of cycles needed to propagate an initiated crack is independent of purity. The highly localized cooperative grain boundary sliding could be more difficult at depressed temperatures. The reason why the *S-N* curve depends on temperature has thus to be primarily sought in temperature dependences of the discussed "localized" mechanism.

4. Conclusions

1. Fatigue behaviour of UFG copper depends on temperature and purity. The temperature dependence for UFG copper is weaker than that for CG copper. The effect of purity is strong for low stress amplitudes (HCF region) and negligible for high stress amplitudes (LCF region).

2. After fatigue loading, no changes of grain morphology were detected by means of TEM and EBSD.

3. After cycling, surface fatigue slip markings along

the traces of the ECAP shear planes were observed.

4. The activity of two concurrent mechanisms of cyclic plastic deformation is considered to be responsible for the observed phenomena: (i) bulk mechanism consisting of irreversible movement of dislocations and (ii) surface mechanism operating in the surface layer consisting of GB sliding along the shear plane of the last ECAP pass.

Acknowledgements

This work was financially supported by the Academy of Sciences of the Czech Republic under the contracts AV0Z20410507 and 1QS200410502. This support is gratefully acknowledged.

References

[1] BESTERCI, M.—KVAČKAJ, T.—KOVÁČ, L.—SÜLLEIOVÁ, K.: Kovove Mater., *44*, 2006, p. 101.
[2] BESTERCI, M.—SÜLLEIOVÁ, K.—KVAČKAJ, T.: Kovove Mater., *46*, 2008, p. 309.
[3] VINOGRADOV, A. Y.—HASHIMOTO, S.: Mat. Trans., *42*, 2001, p. 74.
[4] HÖPPEL, H. W.—KAUTZ, M.—XU, C.—MURASHKIN, M.—LANGDON, T. G.—VALIEV, R. Z.—MUGHRABI, H.: Int. J. Fatigue, *28*, 2006, p. 1001.
[5] MEYERS, M. A.—MISHRA, A.—BENSON, D. J.: Progress in Materials Science, *51*, 2006, p. 427.
[6] GRAY, G. T.—LOWE, T. C.—CADY, C. M.—VALIEV, R. Z.—ALEKSANDROV, I. V.: Nano Structured Mater., *9*, 1997, p. 477.
[7] YU, C. Y.—KAO, P. W.—CHANG, C. P.: Acta Mater., *53*, 2005, p. 4019.
[8] LUKÁŠ, P.—KUNZ, L.—SVOBODA, M.: Met. Mat. Trans., *38A*, 2007, p. 1910.
[9] LUKÁŠ, P.—KUNZ, L.: Mat. Sci. Eng. A, *103*, 1988, p. 233.
[10] BASINSKI, Z. S.—KORBEL, A. S.—BASINSKI, S. J.: Acta Metall., *28*, 1980, p. 191.
[11] KUNZ, L.—LUKÁŠ, P.—SVOBODA, M.: Mat. Sci. Eng. A, *424*, 2006, p. 97.
[12] MURPHY, M. C.: Fatigue Engng. Mater. Struc., *4*, 1981, p. 199.
[13] AGNEW, S. R.—VINOGRADOV, A. Y.—HASHIMOTO, S.—WEERTMAN, J. R.: J. Electronic Mat., *28*, 1999, p. 1038.
[14] MUGHRABI, H.—HÖPPEL, H. W.—KAUZ, M.: Scripta Mat., *51*, 2004, p. 807.
[15] VINOGRADOV, A.—HASHIMOTO, S.—PATLAN, V.—KITAGAWA, K.: Mat. Sci. Eng. A, *319–321*, 2001, p. 862.
[16] MAIER, H. J.—GABOR, P.—KARAMAN, I.: Mat. Sci. Eng. A, *410–411*, 2005, p. 457.
[17] SEEGER, A.: Handbuch der Physik VII/2. Ed.: Flügge, S. Berlin, Springer-Verlag 1958, p. 115.
[18] HOLSTE, C.: Phil. Mag., *84*, 2004, p. 299.
[19] FELTNER, C. E.—LAIRD, C.: Acta Metall., *15*, 1967, p. 1633.